International Journal of Concrete Structures and Materials

RESEARCH Open Access

Experimental Study on Properties of Graphene and Hollow Glass Powder-Added Ultra-High Strength Concrete

Young-Jun Park[1], Hong-Sung Lee[1] and Tae-Seok Seo[1*]

Abstract

A new ultra-high strength concrete, in which oxidized graphene nanoplatelet (GO) and hollow glass powder (HGP) are added, has been developed by authors. This paper presents the material properties of the concrete such as workability, compressive and tensile strengths, internal micro structure (SEM and MIP) as well as air-tightness which was tested using an equipment developed in this study. Test results show that workability and tensile strength significantly increase by a small addition of HGP, and that cGO (GO product of company c) and HGP are well dispersed without agglomeration effect, resulting in more than 20% of reduction in porosity. It is also observed that air-tightness increases by 40% compared with conventional ultra-high strength concrete due to reduction in porosity; thus, new ultra-high strength concrete is anticipated to be effectively used for structures that requires air-tightness such as hyperloop tube. Consequently, it was observed that the workability and mechanical properties of UHSC were increased when cGO and HGP were used instead of silica fume (SF), and authors believe that utilization of new material would contribute to the change in manufacturing method and increase in mechanical properties of concrete.

Keywords Ultra-high strength concrete, Oxidized graphene nanoplatelet, Hollow glass powder, Air-tightness

1 Introduction

Graphene, carbon nano material that a single layer of graphite is peeled off, is widely used in various industry as it has larger specific surface area than any other nano-materials as well as strength, thermal and electric properties are excellent (Kim, 2016). Even small amount of graphene adding to concrete material can contribute effectively to decrease in porosity and increase in mechanical properties with the voids in the concrete matrix filled (Baoguo et al., 2017a, 2017b; Hongjian et al., 2016; Jeong et al., 2019; Nathan et al., 2023; Seo et al., 2015, 2022). Xinyue et al., 2020 and Xinyue et al., 2022 also reported that the graphene is effective for increase in interfacial bond strength at the interfacial transition zone (ITZ) between aggregates and mortar, which is the weakest zone in the concrete. It should be noted that graphene tends to agglomerate among graphene particles due to Van der Waals forces and it does not well disperse in the water because of hydrophobicity (Kim et al., 2014; Seo et al., 2017; Hongjian et al., 2018; Nathan et al., 2023). It is, therefore, very important to increase the dispersion in order for graphene to be used in concrete, hence oxidized graphene nanoplatelet (GO) was developed (Kim, 2016; Youli et al., 2020) which can increase dispersion in high molecular and surface adhesion. However, it is reported that due to high dispersion and large specific surface area of the oxidized graphene, the area of contact becomes larger and water absorption is increased thus molecular behavior of water and superplasticizer is limited, resulting in decrease of workability (Bo et al., 2015; Kim et al.,

Journal information: ISSN 1976-0485 / eISSN 2234-1315

*Correspondence:
Tae-Seok Seo
tsseo75@naver.com
[1] Hyundai Engineering & Construction, Hyundai Bldg. 75, Yulgok-ro, Jongno-gu, Seoul 03058, Korea

2020; Ko et al., 2018). As a result, a solution to solve this problem is required.

As stated above, it is crucial to obtain the workability to apply graphene of nano material to concrete. Yoon et al., (2020) studied the increase of the workability of high strength concrete by mixing with hollow glass powder (HGP) instead of either superplasticizer or silica fume (SF) that is used to increase the workability of conventional high strength concrete. The results show that workability of high strength concrete was increased due to ball bearing effect by small addition of HGP. HGP, made of soda–lime–borosilicate glass, is a micro-powder material with low specific gravity. It is widely used in various areas such as plastic injection and coating material as it is good for reduction in viscosity and increase in fluidity (Yoon et al., 2020).

Based on previous observations above, it is expected that concrete mixed with GO and HGP will contribute to obtaining workability easily and to increasing mechanical properties. In this study, mechanical properties of ultra-high strength concrete mixed with GO and HGP of 120 MPa was studied and the possibility of GO and HGP to replace SF that is essential material used to obtain concrete strength and fluidity was investigated as well.

Some preliminary researches have been performed to use concrete for hyperloop tube (Lim & Park, 2022; Sagong et al., 2021) as the interest in hyperloop of an ultra-high-speed transportation system has increased recently. Since hyperloop is a system that capsules run at ultra-high speed inside the near-vacuum (1 mbar) tube, air-tightness of tube material is very important. In spite of it, studies on the air-tightness of concrete are not sufficient, although Korea Institute of Civil Engineering and Building Technology (2018) conducted experimental research on ultra-high strength concrete. More and various experimental researches on the concrete are required hence ultra-high strength concrete mixed with either SF or GO/HGP were tested using the equipment developed by authors to observe and compare the air-tightness of the ultra-high strength concrete in this study.

2 Overview of Experiment

2.1 Materials and Mix

The material used in this study, cGO, was manufactured by mechanically peeling off expanded graphite in consideration of not only dispersion but economic aspect and then combining with GO. This product is denoted as cGO which means GO manufactured by company c. The cGO was dispersed in superplasticizer to form a superplasticizer dispersion. Since atomization of particles by applying high shear rate (unit: 1/sec) was required to disperse micro particles, a microfludizer at a class of 3.0 kw and 1.0 L/min, which can apply shear rate of 10,000,000 1/sec, was employed to disperse graphene of powder type nano particles. The dispersion was carried out for more than 30 min, and the characteristics of cGO are summarized in Table 1. Fig. 1 shows the concept of cGO and image of cGO taken by Scanning Electron Microscopy (SEM). It is observed from the image that cGO is a plate type structure with irregular convolution and it is reported that such shape was a result of deformation occurred during the peeling off process (Chufa & Murthy, 2020).

The density of HGP used to obtain workability was as low as 0.4 g/cm^3, and specific surface area was very fine as 6000–10,000 cm^2/g. The HGP is a hollow spherical shape outside of which a membrane is formed by a cell composed of soda lime borosilicate glass. Table 2 presents properties of HGP, while Fig. 2 shows an image of HGP taken by SEM. In Table 2, 90% breaking strength of hollow glass powder is defined as the strength at a 10% failure of glass powder by volume under isostatic compression using gas or liquid.

Table 3 summarizes binders and aggregates used in this study; high early strength cement, silica fume, granulated blast-furnace slag and gypsum as binder, and natural silica sand as aggregate. Gypsum ($CaSO_4$) creates ettringite ($C_3A{\cdot}3CaSO_4{\cdot}32H_2O$) by reacting with C_3A in the cement or Al_2O_3 in the Granulated blast-furnace slag. It is known that the expansion of ettringite compensates for the shrinkage of concrete, and furthermore, it is helpful to increase the compressive strength by creating more dense structure. Therefore, a small amount of gypsum is generally used for UHSC of 100 MPa or higher. Two types of concrete mix were employed to investigate the possibility of new ultra-high strength concrete using cGO and HGP as shown in Table 4; a mix portion for ultra-high strength concrete of 120 MPa using SF and the other mix portion using cGO and HGP instead of SF. The amount of cGO mixed was determined to be 1 kg/m^3 based on the observation that increase of strength by input of cGO converges when the input was 1 kg/m^3 (Seo et al., 2022).

2.2 Method of Experiment

2.2.1 Slump Flow and T500

Slump flow was measured following KS F 2594 (2021). T500 is an indirect method to evaluate viscosity of fresh concrete by measuring the required time for slump flow to reach 500 mm.

Table 1 Characteristics of cGO

Layer	Thickness (nm)	Length (μm)	Specific surface area (m^2/g)
5–50	2–20	5–30	50–150

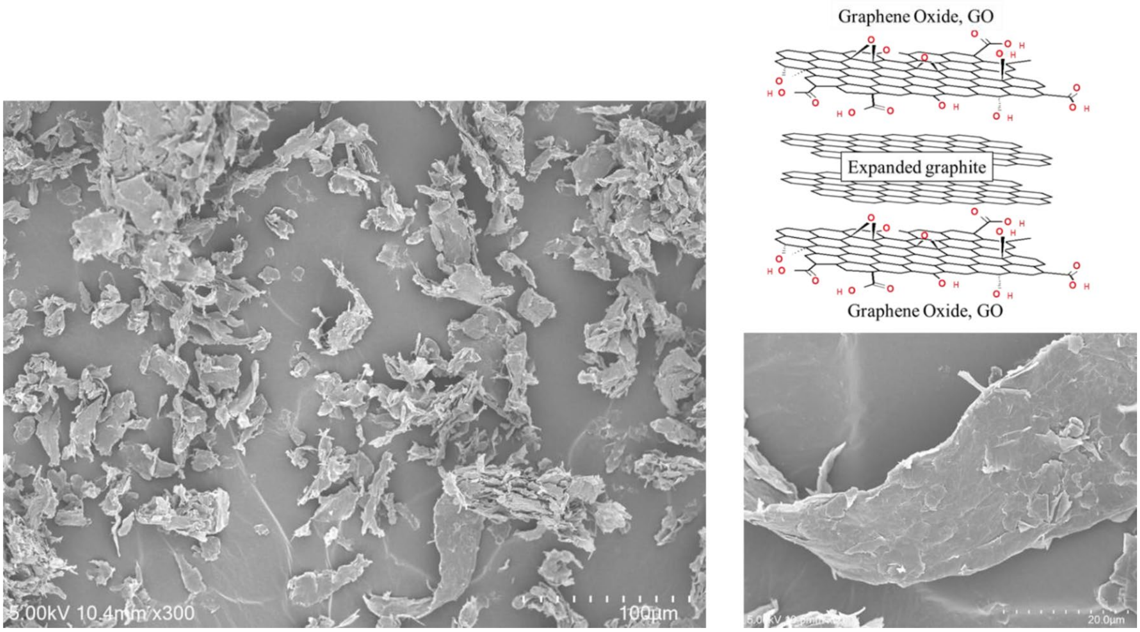

Fig. 1 SEM image of cGO

Table 2 Properties of HGP

Density (g/cc)	90% Breaking strength (MPa)	Particle size distribution (μm, by volume)			
		10th%	50th%	90th%	Effective top size
0.46	110	10	20	20	20

2.2.2 Rheology Test

Rheology of the concrete was measured using an equipment, Rhetribo of company Biel, which can measure yield stress and plastic consistency of fresh concrete. Measurement was conducted; (1) a container of which diameter is 286 mm is filled with concrete, (2) two bladed vane is inserted in the center of the specimen, and the blade is rotated for 20 s at a 0.5 rev/sec, (3) bending moments are measured at an interval of 5 s, total 7 times, while rotation rate is decreased from 0.5 rev/sec to 0.05 rev/sec for 30 s, (4) plastic consistency is finally calculated from the gradient of the line obtained by regression analysis of measure values.

2.2.3 Compressive Strength Test and Splitting Tensile Strength Test

Following KS F 2403 (2005), specimens of Φ100 × 200 mm were prepared to perform strength tests that were conducted for the specimen at 3, 7, and 28 days. Three specimens were casted for each mix portion and standard curing (20 ± 2 ℃, water curing) was employed.

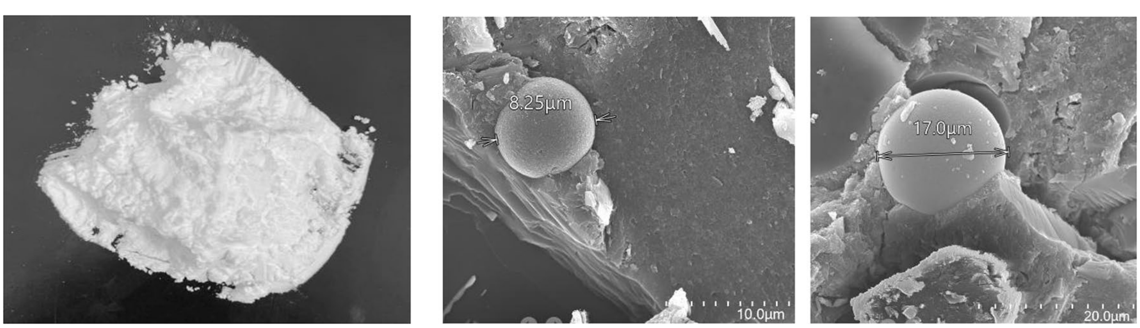

Fig. 2 SEM images of hollow glass powder

Table 3 Properties of materials

Material	Physical properties
Cement (C)	Type III, Specific gravity: 3.15, Specific surface area: 341 m^2/kg
Silica fume (SF)	Specific gravity: 2.20, Specific surface area: 20 m^2/g
Granulated blast-furnace slag (BFS)	Specific gravity: 2.90, Specific surface area: 430 m^2/kg
Gypsum (G)	Specific gravity: 2.81, Specific surface area: 390 m^2/kg
Fine aggregate (S)	Natural silica sand, Specific gravity: 2.62, Particle size: 0.18–0.85 mm
Superplasticizer (SP)	Polycarboxylate high range AE water reducer (liquid type)

Table 4 Concrete mix proportions (ratio by weight)

Mix	W/B (%)	W	C	BFS	SF	G	S	SP (B*%)	cGO (kg/m^3)	HGP (kg/m^3)
Ref	24.0	0.4	1.0	0.5	0.08	0.08	1.88	0.75	–	–
Mix A	24.0	0.4	1.0	0.5	0.08	0.08	1.88	0.75	1.0	–
Mix B	24.0	0.4	1.0	0.5	0.08	0.08	1.88	0.75	1.0	2.0
Mix C	25.3	0.4	1.0	0.5	0.0	0.08	1.98	0.75	1.0	3.0

Mix A: Ref + cGO, Mix B: Ref + cGO + HGP, Mix C: Ref-SF + cGO + HGP

2.2.4 Internal Microstructure (SEM, MIP)

A debris of 10 mm was sampled from the specimen used for strength test, which was then submerged in the acetone for 24 h to stop hydration and dried for another 24 h. SEM (Scanning Electron Microscopy) and MIP (Mercury Intrusion Porosimetry) were carried out to investigate microstructure and porosity, respectively.

2.2.5 Air-Tightness Test

An experimental equipment was developed as shown to investigate the air-tightness of the ultra-high strength concrete developed in this study (Fig. 3). Hollow concrete specimens (ϕ 400 mm, H 500 mm, t 10 mm) with one side closed were casted to be used in the test. A rubber pad was placed between the steel plate and open side of the specimen, while the gap was finished with silicon to prevent external air from going into the specimen through the gap. The vacuum pump hose and a manometer were connected to the upper steel plate to decrease the air pressure inside the specimen and to measure it.

The experiments to evaluate air-tightness of the concrete were performed as follows; (1) the air pressure inside the specimen is decreased down to 1 mbar using a vacuum pump, (2) once the air pressure is reached to the target pressure of 1 mbar, the vacuum pump is turned off, (3) the air pressure slowly increases as the external air infiltrates through the surface of the concrete specimen, (4) the air pressure inside the specimen with time and the required time for air pressure to increase to atmosphere are measured using data logger, and (5) the required times to atmosphere for different materials are compared each other to compare the air-tightness.

3 Results of Experiment and Its Analysis

3.1 Evaluation of Rheology

Changes in slump flow were examined for concretes of different mix portions. The standard mix, denoted as Ref, refers to the one using SF and superplasticizer to obtain workability, while other mixes were obtained by adding cGO and HGP, instead of SF, while unit water contents and amount of superplasticizer were fixed. It was observed that no material segregation occurred from all the mix portions.

The results of slump flow and T500 are shown in Fig. 4. The slump flow of Mix A, in which a 1.0 kg/m^3 of cGO is added to Ref Mix, is 740 mm which decreases by 8% than Ref Mix. T500, from which the viscosity can be indirectly evaluated, also increases by twice (6.9 s) compared with Ref Mix (3.5 s). Such reduction in workability is induced by decrease in performance of superplasticizer as the water absorption increases due to enlargement of contact area between water and graphene having large specific surface area and a good dispersion (Bo et al., 2015; Kim et al., 2020; Ko et al., 2018).

The slump flow was measured for Mix B, where a 2.0 kg/m^3 of HGP is added to Mix A, to evaluate if HGP is effective for improvement of workability. It is observed from the test that HGP workability of Mix A is recovered as flow value increases by more than 4% and T500 decreases by more than 30% than Mix A.

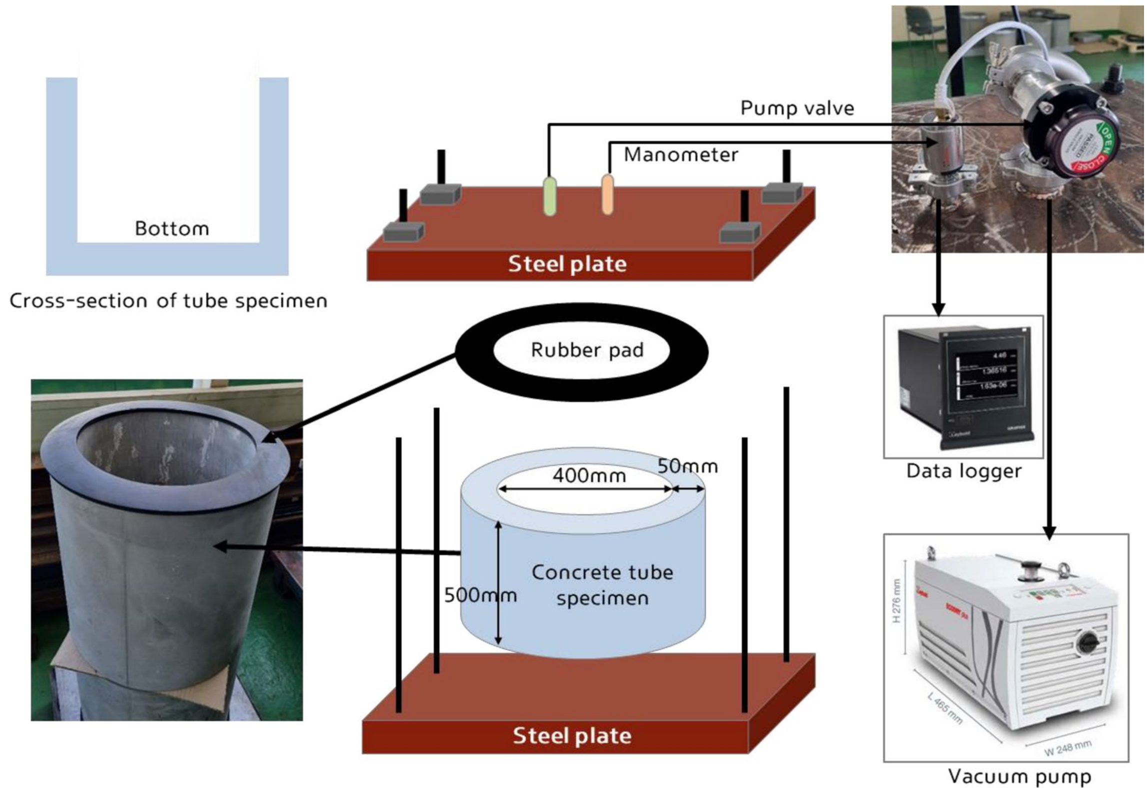

Fig. 3 Air-tightness test equipment

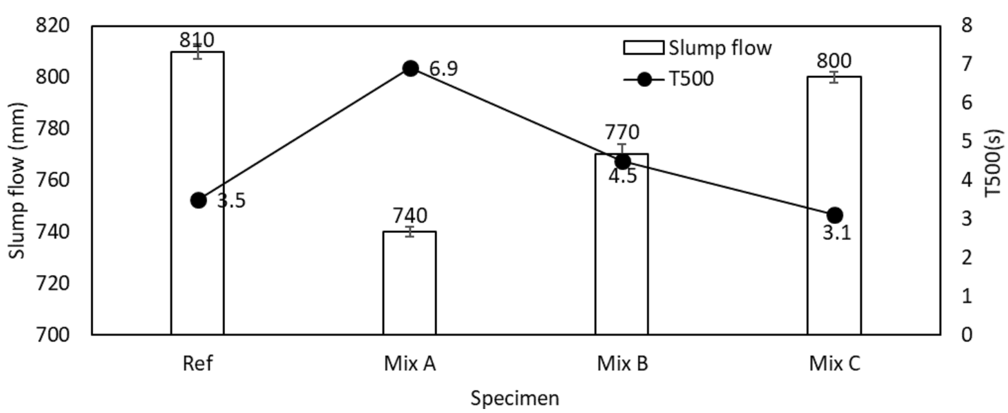

Fig. 4 Results of slump flow and T500 test

In Mix C, cGO and HGP, 1.0 kg/m^3 and 3.0 kg/m^3, respectively, were added instead of SF that is a material essentially used in ultra-high strength to obtain strength and fluidity. Compared with Mix B, additional 1.0 kg/m^3 of HGP was added to Mix C in consideration of viscosity as SF was removed. The results show that slump flow is 800 mm and T500 is 3.1 s, which are almost identical to results of Ref Mix.

Besides slump flow, rheology test was also carried out to measure plastic viscosity and its results are shown in Fig. 5. It is observed that viscosity increases by 3 times more than Ref Mix due to addition of a 1.0 kg/m^3 of cGO but it is recovered by mixing with HGP. In addition to that, it should be noted that HGP plays a great role to significantly recover workability even a small amount (3.0 kg/m^3) of HGP is added to the mix, instead of SF.

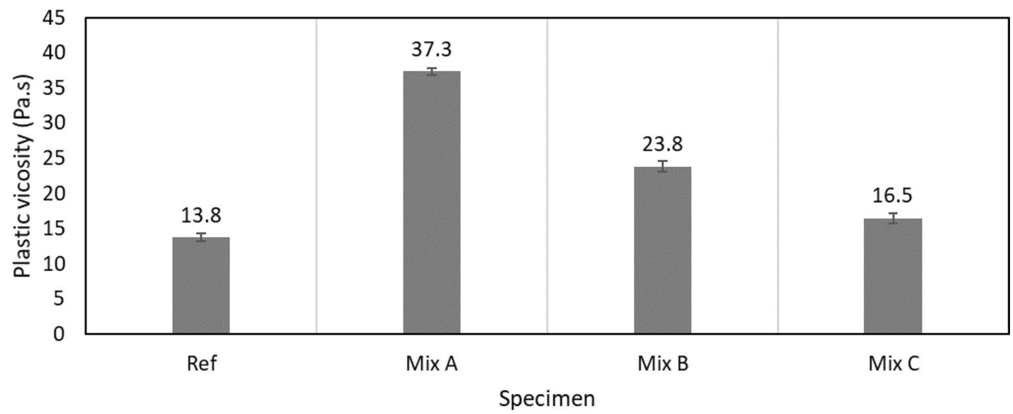

Fig. 5 Evaluation of plastic viscosity

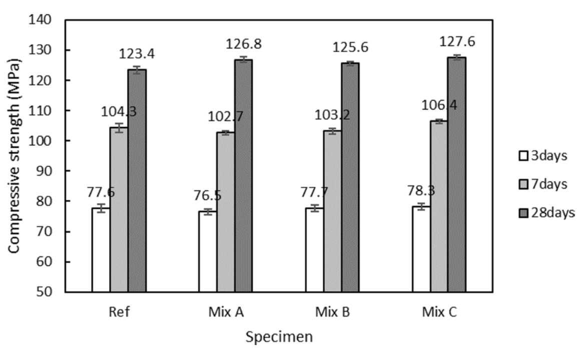

Fig. 6 Results of compressive strength

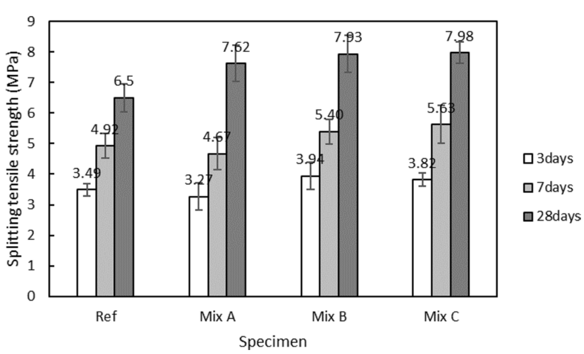

Fig. 7 Results of splitting tensile strength

3.2 Evaluation of Strength

Fig. 6 shows the results of compressive strength tests. The compressive strength obtained from all the mixes are higher than the target strength of 120 MPa. It is also noted that the compressive strengths at 28 days of the concrete mixing with cGO increase by 2 ~ 3% compared with that of Ref concrete that does not contain cGO. Splitting tensile strength was also confirmed to increase by more than 20% in Fig. 7 as cGO was added, and bending strength that was not tested in this study was also reported to increase by 20% (Baoguo et al., 2017b). Since graphene also restrains cracks to propagate just like fibers (Sufen et al., 2020), it is judged that the strength increases due to such restraint. It should be noted that a small amount of cGO, instead of SF, is sufficient for improvement of strength.

3.3 Microstructure (SEM, MIP)

Fig. 8 shows the results of SEM for Mix C specimen. It is visually observed in Fig. 8a that cGO and HGP particles are fairly distributed among hydration products, no agglomeration has occurred. It is also monitored in Fig. 8b that cracks seem to be restrained due to a bridging effect of cGO; thus, tensile strength increases which results from constraint of cracks as reported by Sufen et al., (2020). As shown in Fig. 8c, it is clearly seen that there are no changes in shape or failure in HGP on cracked surfaces. It is assumed, therefore, that improvement of workability is attributed to ball bearing effect due to spherical shape of HGP (Yoon et al., 2020).

Fig. 9 presents the results of MIP analysis conducted on debris taken form Ref specimen and Mix C specimen. In both specimens, pore sizes of 15–25 nm to 25–50 nm are predominant, while overall distribution trend is quite similar each other. With respect to cumulative pore volume, Mix C shows the smaller volume than Ref Mix by 21% (Fig. 9a). Lee et al. (2012) reported that capillary pore could influence the durability of concrete in the negative way as the capillary pore could become infiltration path of carbon dioxide, oxygen, water and so on. Therefore, cumulative pore volume at the range of 0.003–10 µm, which is known as capillary pore range by Kim et al. (2007), were also investigated, and the results show that it also shows smaller value in Mix C than in Ref Mix by 27% (Fig. 9b). It is also reported that porosity could be reduced by up to 40% with the addition of graphene (Sufen et al., 2020). It can be explained that

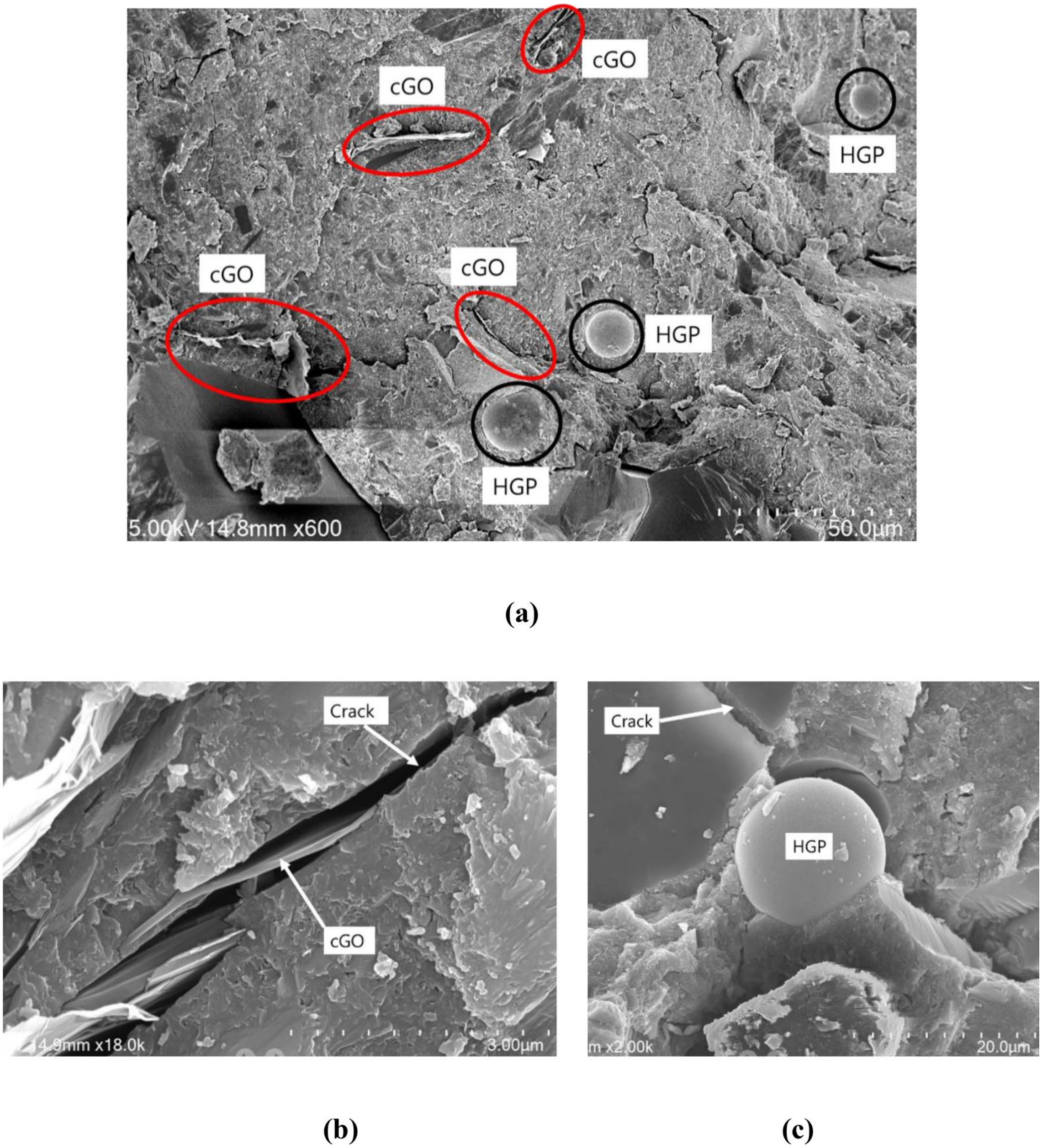

Fig. 8 SEM image of concrete enriched with cGO and HGP: **a** cGO and HGP inside concrete; **b** cGO on cracked surface; **c** HGP on cracked surface

very small size particles of graphene having high specific surface area like cGO can contribute to the decrease in porosity as graphene is excellent for filling the voids in the concrete matrix (Baoguo et al., 2017a).

3.4 Evaluation of Air-Tightness

Fig. 10 shows the schematic diagram of pressure change inside the tube specimen during air-tightness test. As previously mentioned, the internal pressure of the specimen was decreased down to 1 mbar using a vacuum pump, and recovery time for pressure to rise up to atmosphere was measured during which the vacuum pump was turned off. Three mix portion types of concrete tube specimens were prepared and tested to evaluate air-tightness, which were Ref Mix concrete, Mix C concrete having 1.0 kg/m^3 of graphene, and Mix C+cGO(0.2) concrete adding additional 0.2 kg/m^3 of graphene to Mix C (i.e. total amount of graphene was 1.2 kg/m^3).

The air-tightness of Mix C specimen, indirectly evaluated using recovery time, increased by 40% more

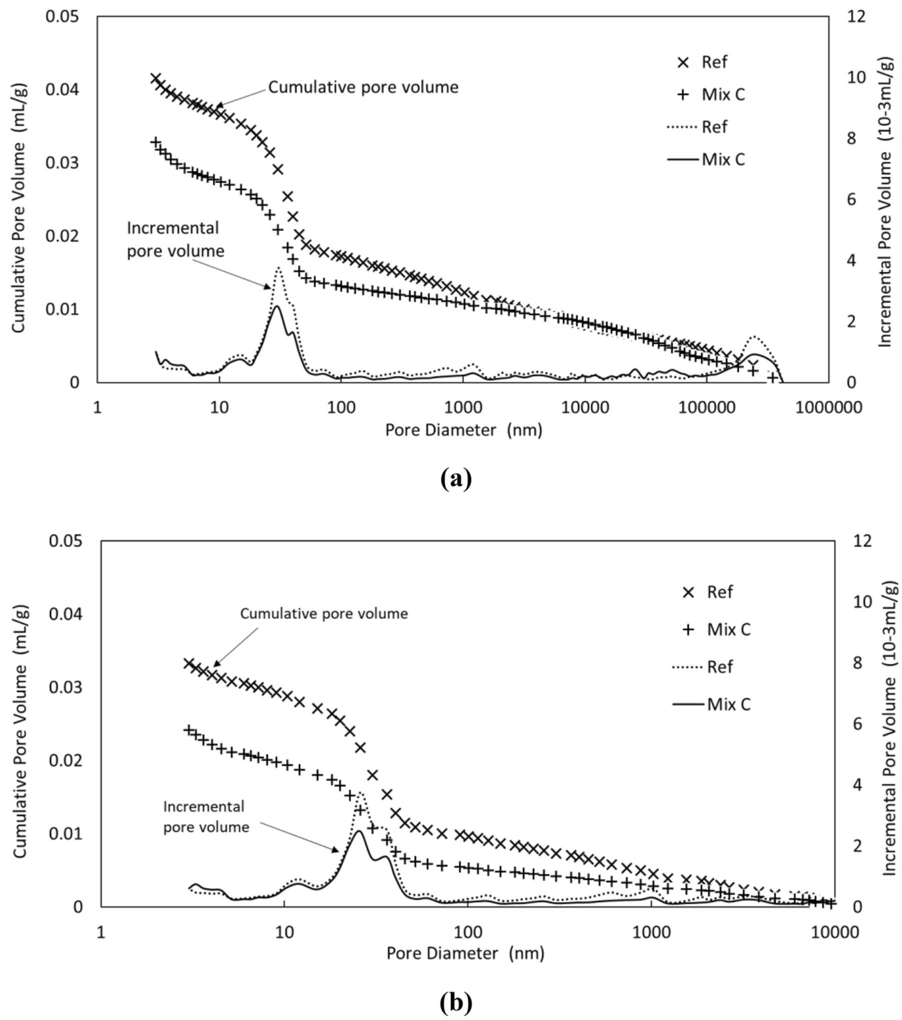

Fig. 9 Results of MIP analysis: **a** pore size distribution and total cumulative pore volume; **b** pore size distribution and total cumulative capillary pore volume

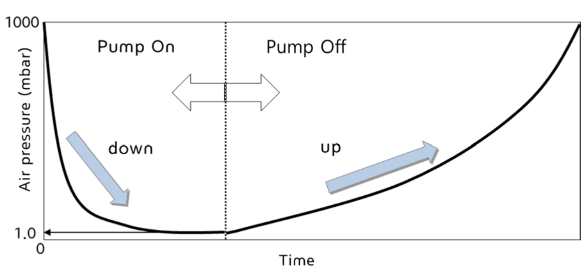

Fig. 10 Schematic diagram of air pressure change in concrete tube specimen

compared with that of Ref specimen, as shown in Fig. 11. As confirmed in MIP analysis, such increase of air-tightness were obtained as a result of decrease in porosity as graphene having large specific surface area and two dimensions shape was well dispersed inside the concrete specimen. As a result of the air-tightness test of Mix C and Mix C + cGO (0.2), the recovery time from 0.001 atm to 1 atm was 113.5 min and 108.4 min, respectively, showing no improvement in air-tightness performance, although amount of graphene increased in Mix C + cGO.

Considering the influence of graphene on concrete strength, air-tightness and economic aspect, it is judged that optimum amount of graphene to be added is around 1.0 kg/m^3, although collection of more data in various conditions is required to verify this. Based on the observation, it is considered that, due to its lower porosity, the ultra-high strength concrete newly developed in this study can be used for such structures as hyperloop that requires excellent air-tightness. Followed by the study presented in this paper, the authors are to perform

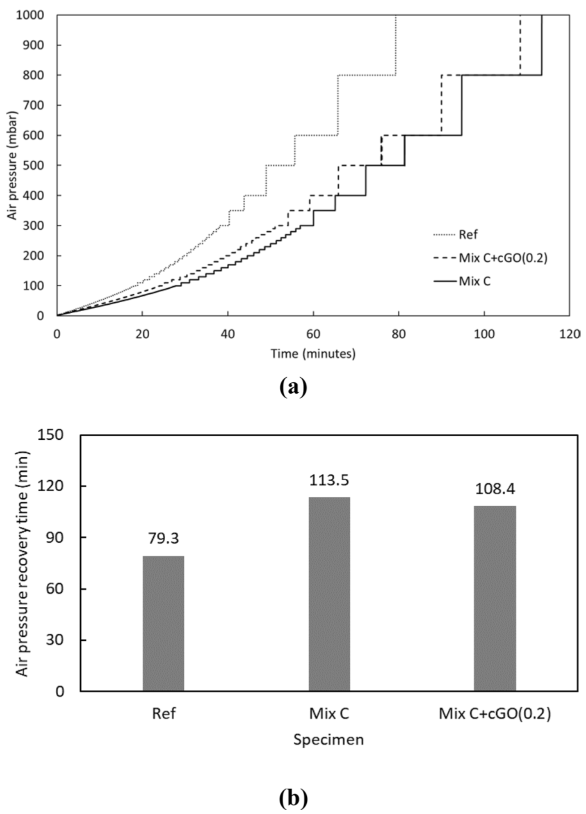

Fig. 11 Test results of air-tightness test: **a** behavior of air pressure in concrete specimen; **b** comparison of air pressure recovery time

additional research on methods to advance the air-tightness of the ultra-high strength concrete.

4 Conclusions

Mechanical properties of ultra-high strength concrete using cGO and HGP were investigated in this study, and following observations have been obtained.

1. Workability was examined for Ref Mix that already obtained workability using SF and superplasticizer, but SF was replaced by cGO and HGP in this study. The workability became as very poor as the work was almost impossible by addition of 1.0 kg/m^3 of cGO, however, it was confirmed that the workability was recovered equivalent to or better than Ref Mix when 2.0–3.0 kg/m^3 of HGP was added resulting in increase in fluidity and decrease in viscosity.
2. It was observed that the compressive strength and splitting tensile strength at 28 days increased by 3% and 20%, respectively. It is reported that graphene is effectively restrains cracks to propagate, therefore, it is understood that the strength of the concrete increases due to such effect of graphene.
3. The results of SEM show that cGO and HGP particles are fairly distributed among hydration products, no agglomeration is detected. It was also observed that cGO seemed to act as a bridge on cracked surface. Neither change in shape nor failure of HGP on cracked surfaces occurred as well. It is assumed that improvement of workability is attributed to ball bearing effect due to spherical shape of HGP.
4. With respect to the cumulative pore volume, Mix C shows the smaller volume than Ref Mix by 21%, and the cumulative pore volume at the capillary pore range of 0.003 to 10 μm was also smaller by 27% for Mix C than for Ref Mix.
5. The results of air-tightness test show that air-tightness of Mix C specimen is higher by 40% than Ref Mix specimen. This is due to that two-dimensional plate shaped graphene is well dispersed in the concrete; thus, porosity decreases.
6. The recovery time from 1 mbar to atmosphere are 113.5 min and 108.4 min for Mix C and Mix C + cGO(0.2), respectively, which shows no meaningful difference from different amount of graphene added.

Acknowledgements
Not applicable.

Author contributions
Y-JP planned the test and wrote mainly the paper; H-SL performed the tests and organized the test results; T-SS is a principal investigator of the research project and proposed the main idea of the research. All authors read and approved the final manuscript.

Funding
Not applicable.

Availability of data and materials
All data generated or analyzed during this study are included in this published article.

Declarations

Ethics approval and consent to participate
Not applicable.

Consent for publication
All the authors agree that the article will be published after acceptance.

Competing Interests
The authors declare that they have no competing interests.

Received: 12 December 2023 Accepted: 7 February 2024
Published online: 13 July 2024

References

Baoguo, H., Liqing, Z., Shuzhu, Z., Sufen, D., Xun, Y., Rongwei, Y., & Jinping, O. (2017a). Nano-core effect in nano-engineered cementitious composites. *Composites Part a: Applied Science and Manufacturing, 95*, 100–109.

Baoguo, H., Qiaofeng, Z., Shengwei, S., Sufen, D., Liqing, Z., Xun, Y., & Jinping, O. (2017b). Enhancing mechanisms of multi-layer graphenes to cementitious composites. *Composites Part a: Applied Science and Manufacturing, 101*, 143–150.
Bo, Z., Shu, J. C., Asghar, H. K., Frank, C., Wang, C. M., & Wen, H. D. (2015). Effect of ultrasonication energy on engineering properties of carbon nanotube reinforced cement pastes. *Carbon, 85*(4), 212–220.
Chufa, B. M., & Murthy, H. C. A. (2020). Effect of reinforcement of reduced graphene oxide on mechanical properties of concrete nanocomposite. *Journal of Materials and Environmental Science, 11*(6), 844–855.
Hongjian, D., Hongchen, J. G., & Sze, D. P. (2016). Improvement in concrete resistance against water and chloride ingress by adding graphene nanoplatelet. *Cement and Concrete Research, 83*, 114–123.
Hongjian, D., & Sze, D. P. (2018). Dispersion and stability of graphene nanoplatelet in water and its influence on cement composites. *Construction and Building Materials, 167*, 403–413.
Jeong, SH., Kim, DU., Lee, SJ., & Won, JP. (2019). Mix proportion of graphene cement composites. Proceedings of the Korea Concrete Institute. 501–502.
Kim, H. K., Nam, I. W., & Lee, H. K. (2014). Enhanced effect of carbon nanotube on mechanical and electrical properties of cement composites by incorporation of silica fume. *Composite Structures, 107*(1), 60–69.
Kim, J. H., Choi, I. J., Kim, S. H., Han, S. Y., & Joung, C. W. (2020). Production of graphene oxide reinforced cement paste. *Building Construction, 20*(2), 39–44.
Kim, K. N. (2016). Technology development trend and application of graphene. *Korean Institute of Electrical and Electronic Material Engineers, 29*(6), 3–11.
Kim, N. W., Yeo, D. G., Song, J. H., & Bae, J. S. (2007). A study on the characteristic of capillary pore and chloride diffusivity by electrical difference of high strength concrete using metakaolin. *Journal of Korea Concrete Institute, 19*(4), 499–506.
Ko, HJ., Choi, BK., Park, YK., Yoon, JY., & Yoon, GW. (2018). The physical properties mortar by graphene oxide mixing method. Proceedings of the Korea Concrete Institute, 539–540.
Korea Institute of Civil Engineering and Building Technology (2018). Research on infrastructures technologies for next generation hyper speed transportation system. Annual Report Of Internal Research Project. 42–46.
KS F 2403. (2005). *Method of making and curing concrete specimens*. Seoul: Korea Agency for Technology and Standards.
KS F 2594. (2021). *Method of test for slump flow of fresh concrete*. Seoul: Korea Agency for Technology and Standards.
Lee, C. L., Huang, R., Lin, W. T., & Weng, T. L. (2012). Establishment of the durability indices for cement-based composite containing supplementary cementitious materials. *Materials and Design, 37*, 28–39.
Lim, JO., & Park, JN. (2022). Evaluation of airtightness performance on prestressed and circular confined concrete tube structures. Proceedings of the Korea Concrete Institute. 69–70.
Nathan, J. E., Youli, L., Hongjian, D., & Dong, R. (2023). Effect of graphene oxide on cement mortar under quasi-static and dynamic loading. *Journal of Building Engineering, 74*, 106783.
Sagong, M., Seo, G. S., Kim, L. H., Park, K. P., Kim, M. C., Yeo, I. H., & Lee, K. S. (2021). Development and evaluation of concrete tube the hyper tube express. *Journal of the Korean Society for Railway, 24*(7), 634–645.
Seo, KS., Song, YM., Choi, WS., & Chung, WS. (2015). Effect of some parameters on the compressive strength of graphene oxide cement composites. Proceedings of Korea Concrete Institute. 553–554.
Seo, TS., Lee, HS., & Kim, KM. (2022). Experimental study on the properties of UHPC mixed with graphene. Proceedings of the Korea Institute of Building Construction. 199–200.
Seo, W. W., Kim, G. Y., Yoon, M. H., Lee, B. K., & Nam, J. S. (2017). Mechanical properties of epoxy paint using oxidized graphene nanoplatelet as a reinforcement. *Journal of Korea Institute of Building Construction, 17*(5), 465–471.
Sufen, D., Yanlei, W., Ashraf, A., Baoguo, H., & Jinping, O. (2020). Nano/microstructures and mechanical properties of ultra-high performance concrete incorporating graphene with different lateral sizes. Composites Part A. *Applied Science and Manufacturing*. https://doi.org/10.1016/j.compositesa.2020.106011
Xinyue, W., Sufen, D., Ashraf, A., Wei, Z., & Baoguo, H. (2020). Effect and mechanisms of nanomaterials on interface between aggregates and cement mortars. *Construction and Building Materials, 240*, 117942.
Xinyue, W., Sufen, D., Zhenming, L., Baoguo, H., & Jinping, O. (2022). Nanomechanical characteristics of interfacial transition zone in Nano-engineered concrete. *Engineering, 17*, 99–109.
Yoon, S., Lee, H. Y., & Seo, T. S. (2020). Experimental study on the material properties of high strength concrete with hollow glass powder. *Journal of the Korea Institute of Building Construction, 20*(4), 313–319.
Youli, L., & Hongjian, D. (2020). Graphene reinforced cement composites: A review. *Construction and Building Materials, 265*, 120312.

Publisher's Note

Young-Jun Park Vice president, PhD, Hyundai Engineering & Construction, Hyundai Bldg. 75, Yulgok-ro, Jongno-gu, Seoul, 03058, Korea

Hong-Sung Lee Senior researcher, PhD, Hyundai Engineering & Construction, Hyundai Bldg. 75, Yulgok-ro, Jongno-gu, Seoul, 03058, Korea

Tae-Seok Seo Senior researcher, PhD, Hyundai Engineering & Construction, Hyundai Bldg. 75, Yulgok-ro, Jongno-gu, Seoul, 03058, Korea